



UNIVERSITY  
OF FERRARA

- EX LABORE FRUCTUS -

2<sup>nd</sup> International Seminar on ORC Power Systems

October 7<sup>th</sup> & 8<sup>th</sup>, 2013

De Doelen, Rotterdam, NL

# GEOMETRIC, THERMODYNAMIC AND CFD ANALYSES OF A REAL SCROLL EXPANDER FOR MICRO ORC APPLICATIONS

**M. Morini, C. Pavan, M. Pinelli,  
E. Romito, A. Suman**

Dipartimento di Ingegneria  
Università degli Studi di Ferrara (Italy)

# Introduction

The **ORC systems** are becoming more common for the exploitation of energy sources with low enthalpy and for a **very small power** application (<10 kWe)

The **Scroll** fluid machine seems to be suitable for this applications thanks to:

- small number of moving parts
- low noise and vibrations
- good dynamic performance

Some of the main challenges for scroll enhancement

- *High efficiency*  
*CFD* simulations could represent a very “new” *useful method*
- *Low cost*  
*Commercial devices* could represent a good starting solution



**Sanden TRSA09-3658**

**Integrated** approach with **CFD Analyses** on **commercial devices** can allow the achievement of new knowledge and on the optimization of scroll technology



# State of the art

Researchers	Expander type	Working fluids	Isentropic efficiency (%)	Power [kW]	Rotate speed [rpm]	Pressure ratio
Yamamoto et al. [150]	Radial-inflow turbine	R123	48	0.15	17,000	-
Nguyen et al. [151]	Radial-inflow turbine	<i>n</i> -pentane	49.8	1.44	65,000	3.45
Yagoub et al. [152]	Radial-inflow turbine	HFE-301	85	1.50	60,000	1.1
		<i>n</i> -pentane	40	1.50	60,000	1.3
Inoue et al. [153]	Radial-inflow turbine	TFE	70–85	5–10	15,000–30,000	4.8
Kang [154]	Radial-inflow turbine	R245fa	78.7	32.7	63,000	4.11
Pei et al. [155]	Radial-inflow turbine	R123	65	1.36	24,000	5.2
Li et al. [156]	Radial-inflow turbine	R123	68	2.40	40,000	6.3
Zanelli and Favrat [157]	Scroll expander	R134a	63–65	1–3.5	2400–3600	2.4–4.0
Mathias et al. [158]	Scroll expander	R123	67, 81, 83	1.2, 1.38, 1.75	3670	8.8, 5.5, 3.1
Peterson et al. [159]	Scroll expander	R123	45–50	0.14–0.24	600–1400	3.28–3.87
Wang et al. [88]	Scroll expander	R134a	70–77	0.5–0.8	1015–3670	2.65–4.84
Saitoh et al. [160]	Scroll expander	R113	65	0–0.46	1800–4800	-
Kim et al. [161]	Scroll expander	Water	33.8	11–12	1000–1400	10.54–11.5
Manolakos et al. [162]	Scroll expander	R134a	10–65	0.35–2	300–390	-
Lemort et al. [86,87]	Scroll expander	R123	42.5–67	0.4–1.8	1771–2660	2.75–5.4
	Scroll expander	R245fa	45–71	0.2–2	-	2–5.7
Guangbin et al. [163]	Scroll expander	Air	-	0.4–1.1	1740–2340	3.66
Wang et al. [164]	Screw expander	Air	26–40	0.5–3	400–2900	-
Smith et al. [165]	Screw expander	R113	48–76	6–15.5	1300–3600	2.11
Baek et al. [166]	Reciprocating piston expander	CO <sub>2</sub>	10.5	24.35	114	2.1
Zhang et al. [167]	Reciprocating piston expander	CO <sub>2</sub>	62	-	306	2.4
Mohd et al. [101]	Rotary vane expander	R245fa	43–48	0.025–0.032	2200–3000	21.54–24.17
Yang et al. [102]	Rotary vane expander	CO <sub>2</sub>	17.8–23	-	300–1500	-
Qiu et al. [168]	Rotary vane expander	HFE7000	52.88–55.45	1.66–1.72	841–860	2.063–2.095

**Scroll expander → up to 2 kW**



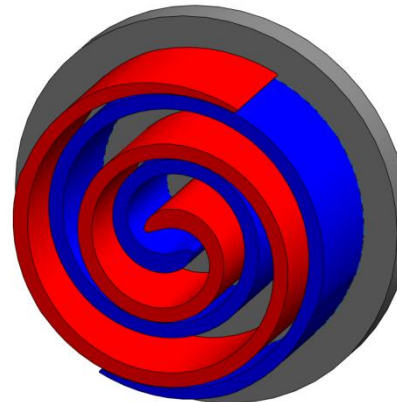
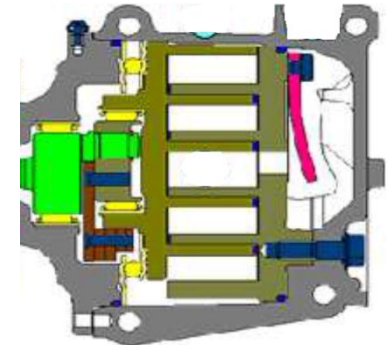
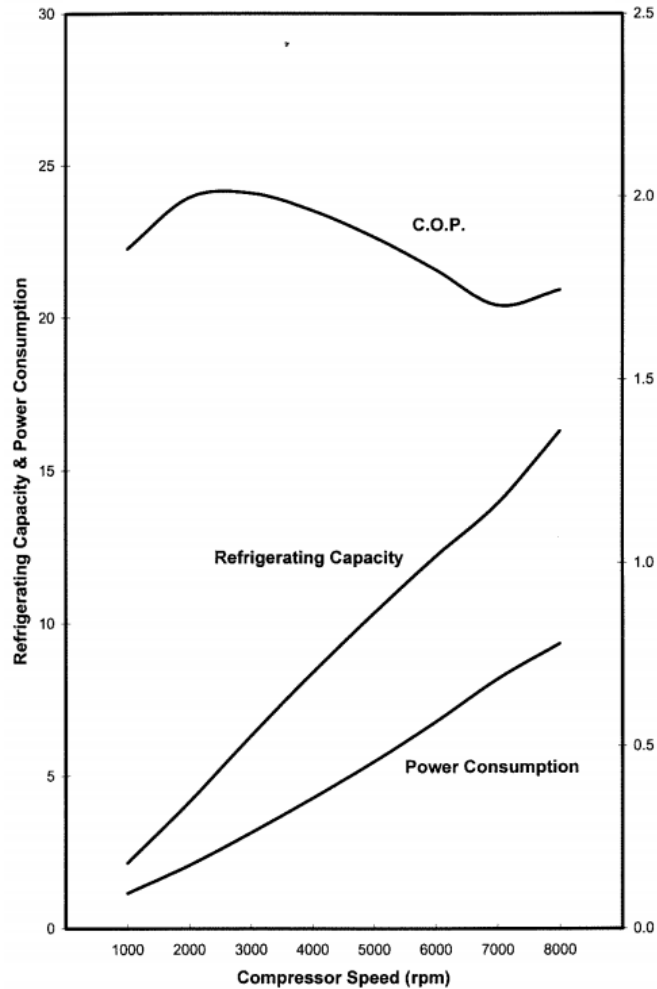
# Objectives

- Acquisition of the scroll compressor Sanden TRSA09-3658 (A/C automotive compressor) geometry through a Reverse Engineering procedure
- Set-up of the transient simulation, with a Dynamic Mesh strategy of the scroll in compression and expansion operations
- Comparison between the CFD results and the results obtained by a simplified thermodynamic model
- Analysis of the performance in terms of pressure and mass flow rate profiles and volumetric efficiency

# Sanden TRSA09-3658 features

## TRSA09 Performance

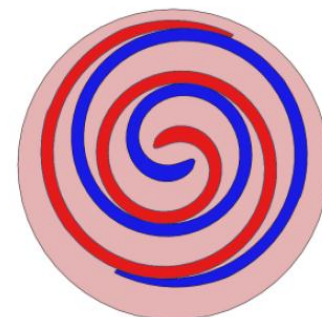
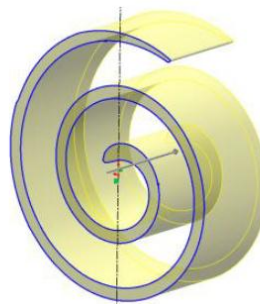
Pressure Dis / Suc : 1.67(MPa) / 196(kPa) [gage]  
Sub Cool / Super Heat : 0 / 10(K)



- A/C Automotive compressor
- Rot. Speed: max 10,000 rpm
- End plate  $\approx$  120 mm
- Volumetric Ratio = 3.1055

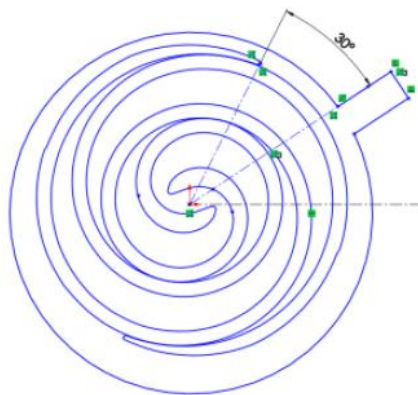
# Reverse Engineering procedure (1)

- The RE procedure was performed by means of a 7320 Romer laser scanner
- Subsequent parametric CAD reconstruction was obtained by Interpolating the point cloud derived from the laser scanner by means of the Polyworks software in order to obtain the 3D polygonal model



# Reverse Engineering procedure (2)

- 2D section has been obtained by perpendicular planes with respect to the orbit axis in order to obtain an exportable 2D section
- The scroll profile is then made regular and continuous by means of Spline curves



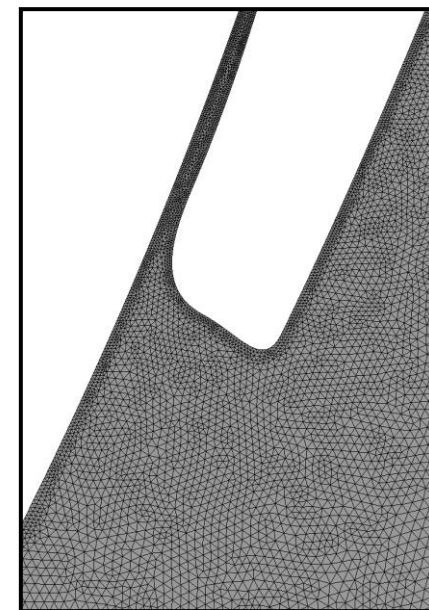
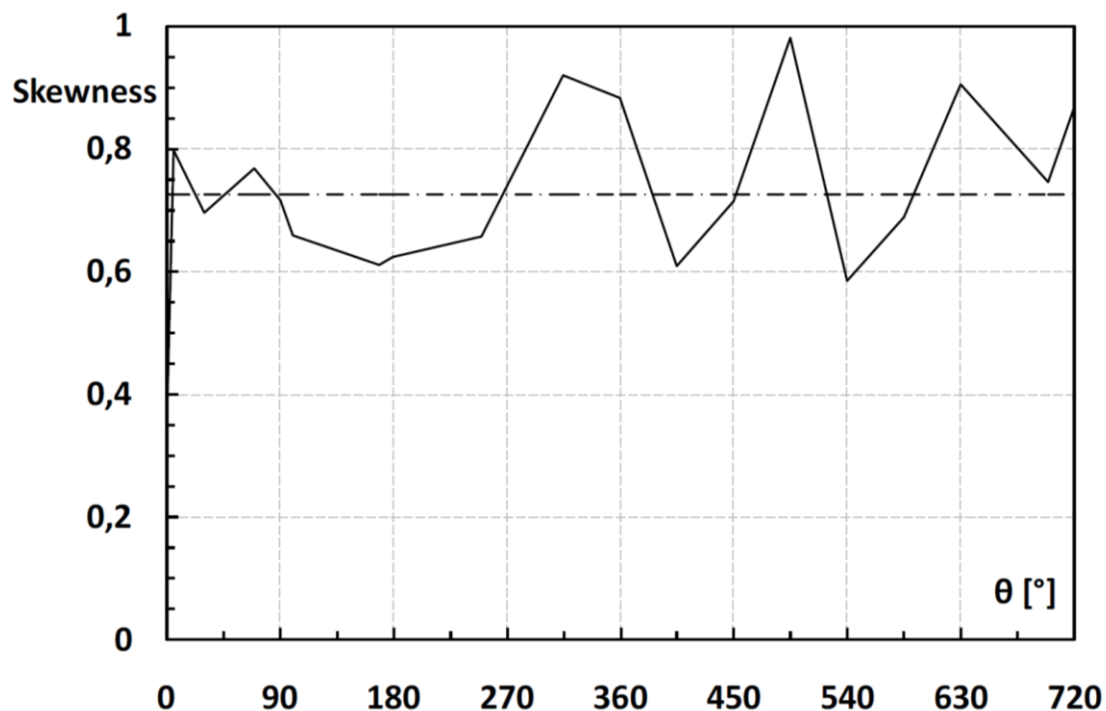
- The flank gaps for the RE geometry are function of the crank angle (non constant gaps during rotation)

Position	Max. gap [ $\mu\text{m}$ ]
0° (*)	20
90°	36
180°	180
270°	36

(\*)inlet chambers close

# CFD – Mesh

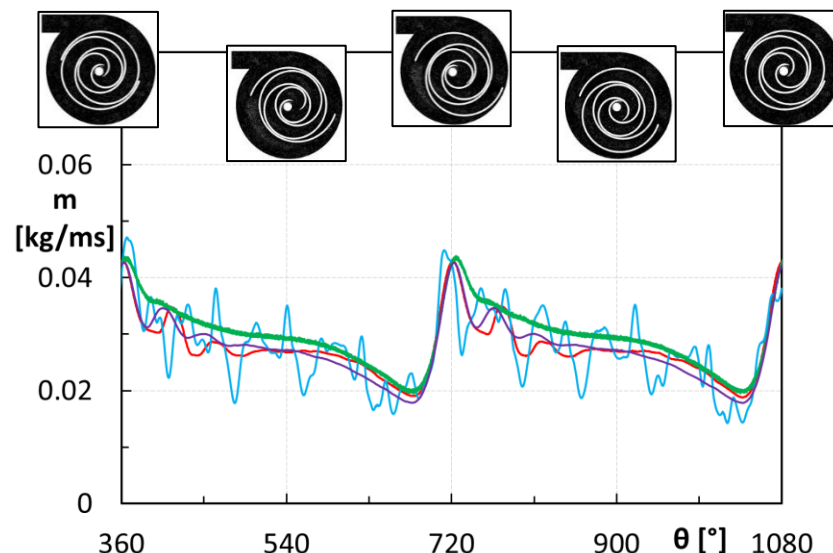
- 2D domain - from RE geometry
- Mesh - with *local refinement*
- Grid point - 755 770 tetrahedral elements regenerated each time step
- Skewness monitored and controlled at each time step
- Min Orthogonal Quality > 0.66



- ANSYS Fluent numerical code
- Working fluid air as a perfect gas
- k- $\epsilon$  turbulence model with standard wall functions  
*proved to be quite robust in the near gap and gap zones where local Reynolds number can decrease appreciably*
- 2D transient simulations by using a **Dynamic Mesh** strategy  
*can reproduce the real operation of the machine through a sequence of different positions by imposing an angular increment  $\Delta\theta$*
- The  $\Delta\theta$  influence the *local solution* and the *quantity fluctuation* during the spiral rotation. From previous analysis\*

$$\Delta\theta = 0.0625^\circ$$

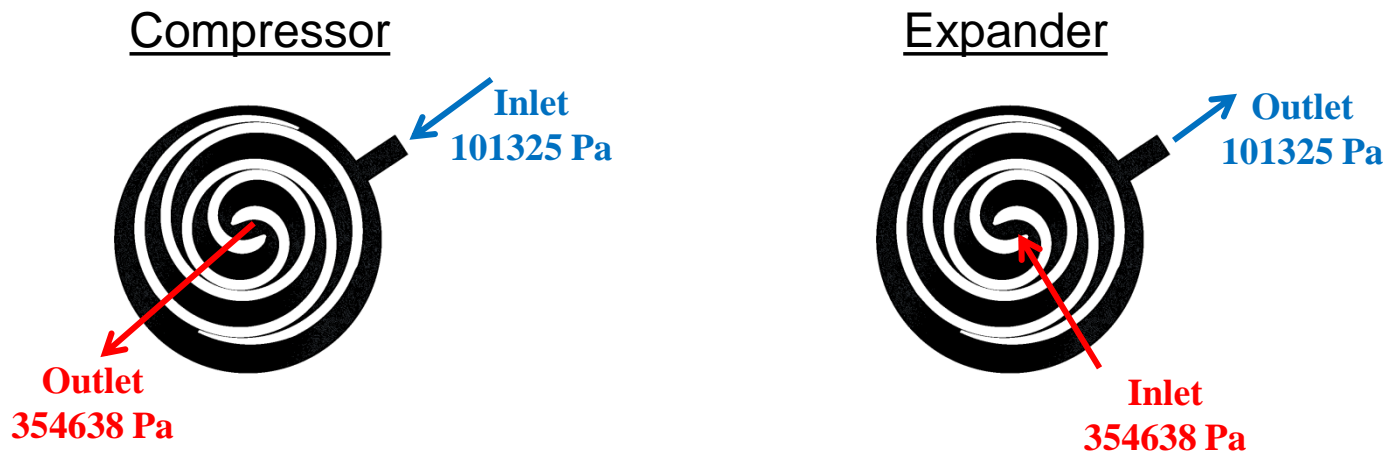
- $\Delta\theta = 0.2500^\circ$    ●  $\Delta\theta = 0.1250^\circ$
- $\Delta\theta = 0.0625^\circ$    ●  $\Delta\theta = 0.0417^\circ$



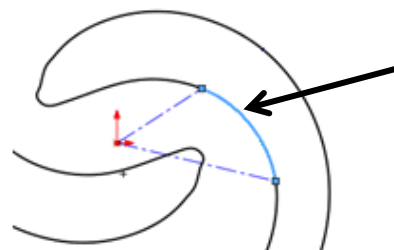
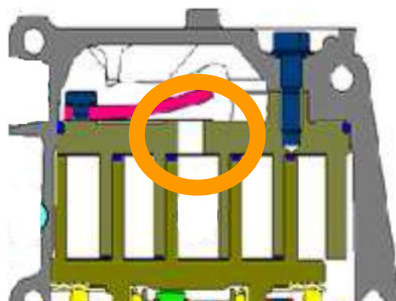
\* Morini, M., Pavan, C., Pinelli, M., Romito, E., Suman, A., "Modeling of scroll machines: geometric, thermodynamics and CFD methods", ASME ORC 2013, Oral presentation

# CFD – Boundary Conditions

- Differentiated between compression and expansion operation



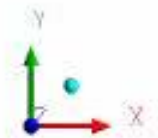
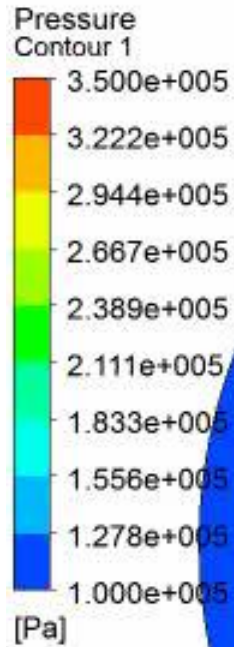
- Outlet (compressor) or inlet (expansion) section is radial
- Since a 2D domain is considered, a numerical simplification was adopted for the outlet/inlet section



Outlet/Inlet section obtained on the fixed profile



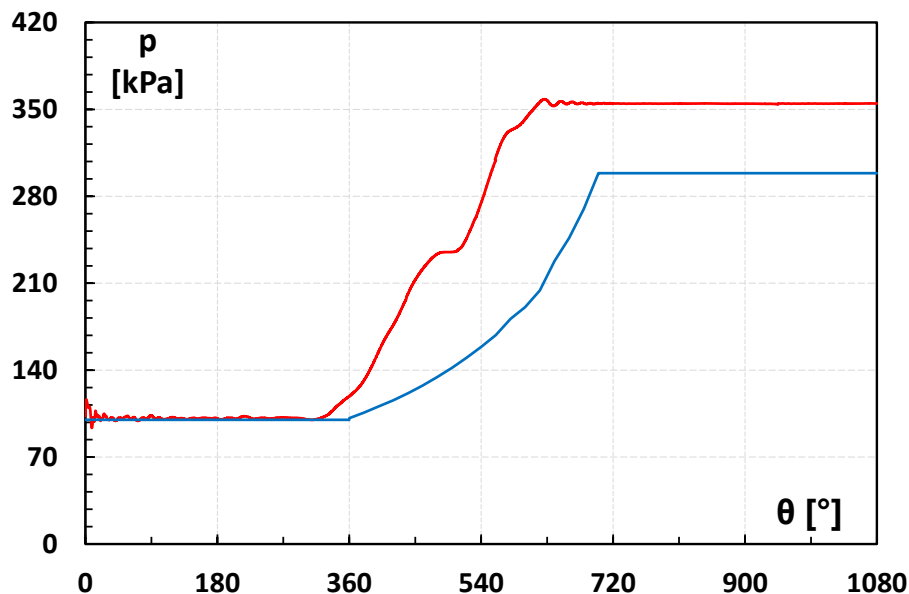
# CFD – Pressure



# Comparison: CFD vs. thermodynamic

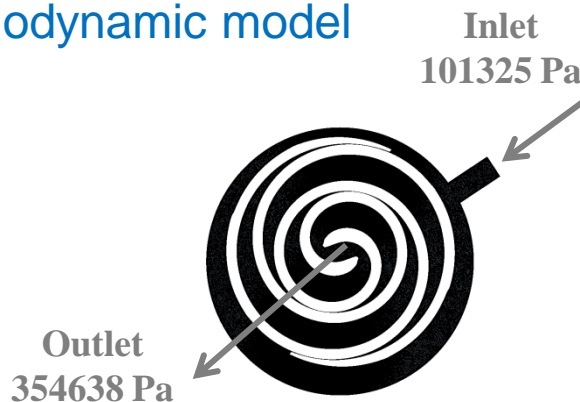
- Simplified thermodynamic model of an energy balance in an open control volume:
  - no heat exchange
  - constant fluid properties at inlet and outlet sections
  - air ideal gas @ standard conditions
  - partial derivatives approximated by finite differences

$$\frac{\Delta T}{\Delta \theta} = \frac{1}{m c_v} \left\{ -T \left( \frac{\Delta p}{\Delta T} \right)_v \frac{\Delta V}{\Delta \theta} \right\} = \frac{1}{c_v} (-T) R \frac{1}{V_c} \frac{\Delta V_c}{\Delta \theta}$$



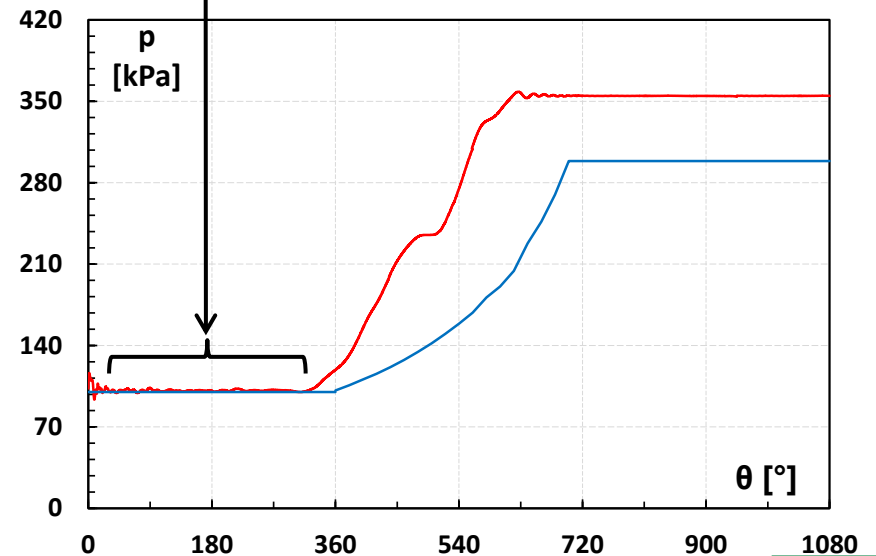
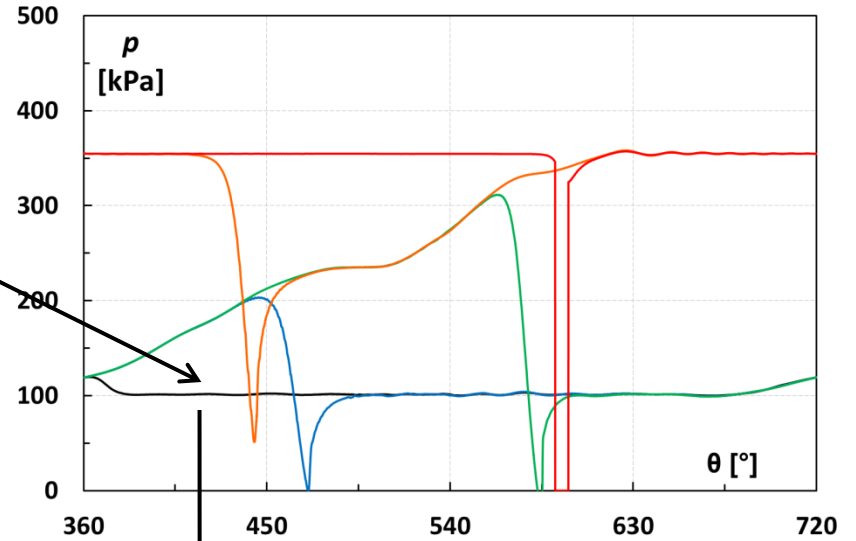
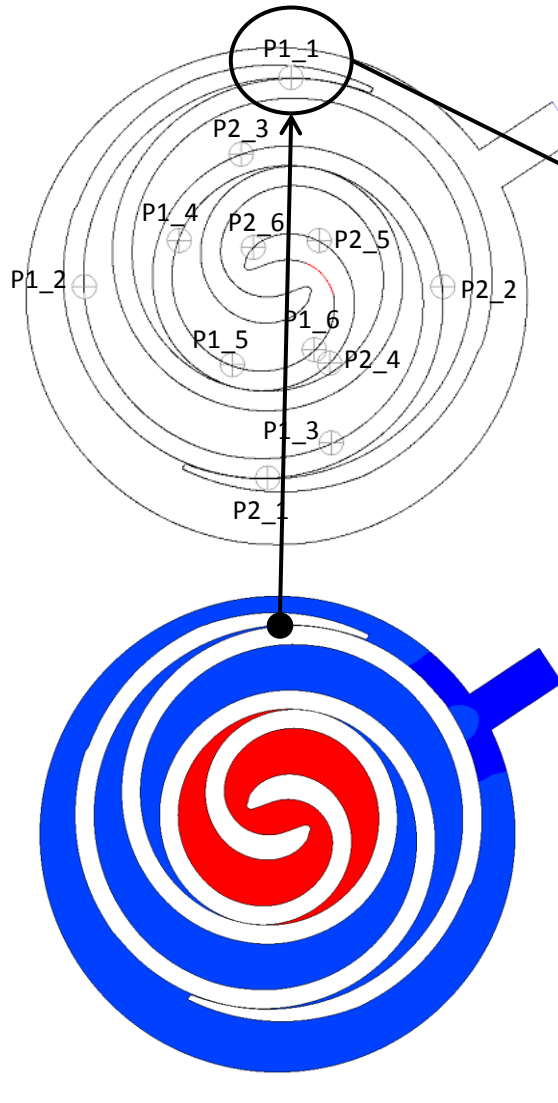
CFD Results

Thermodynamic model



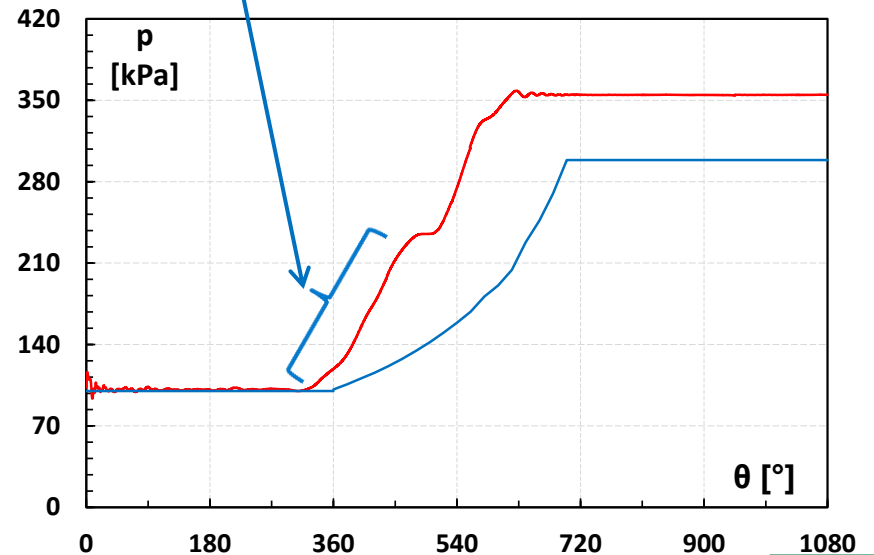
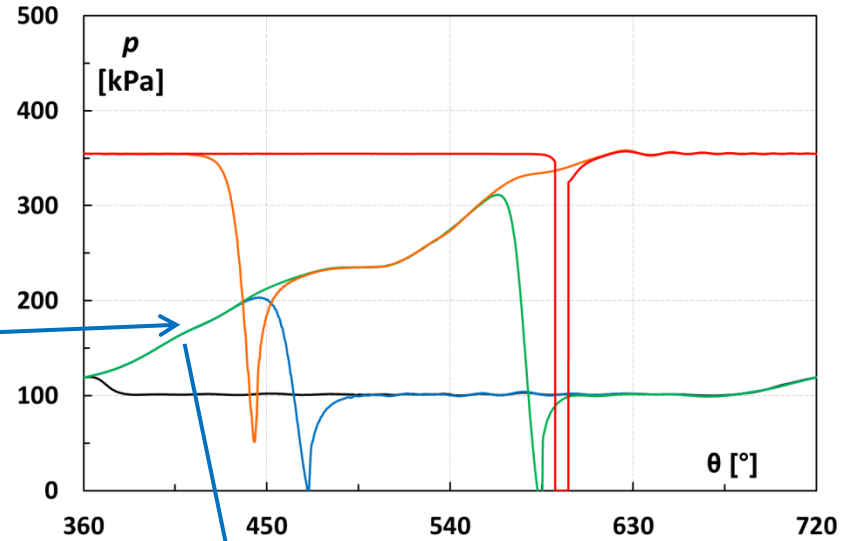
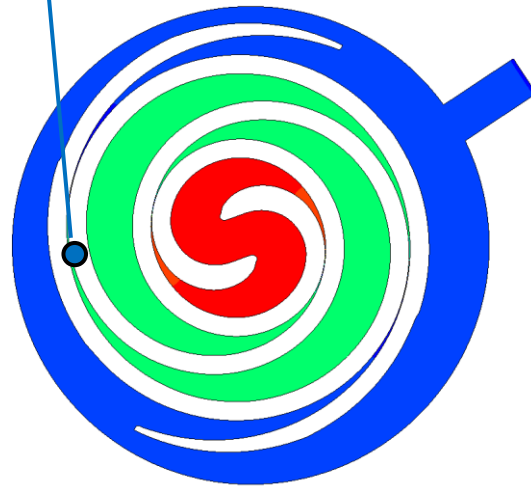
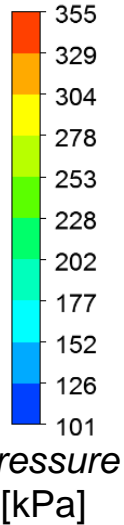
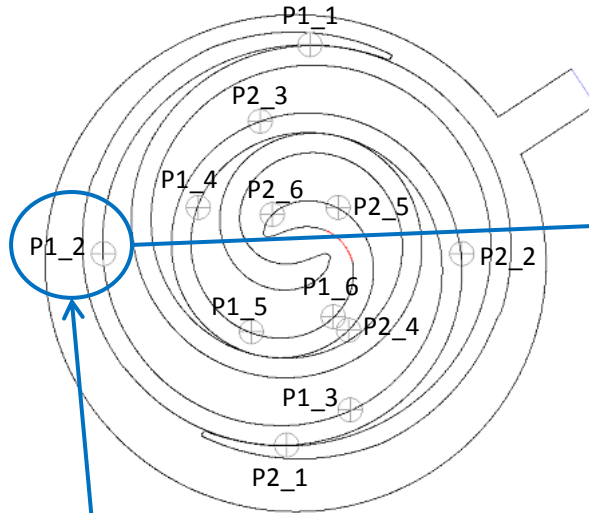
# Pressure control point (1)

## Compressor suction chamber 1



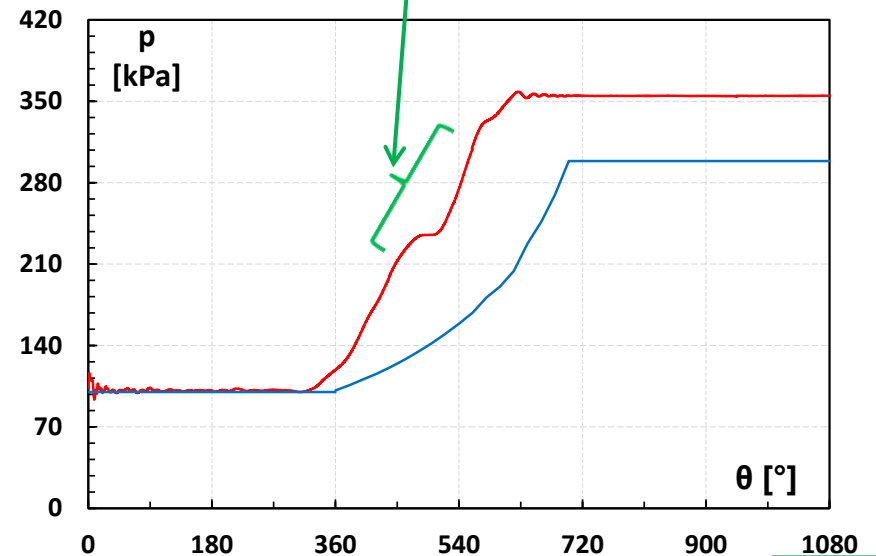
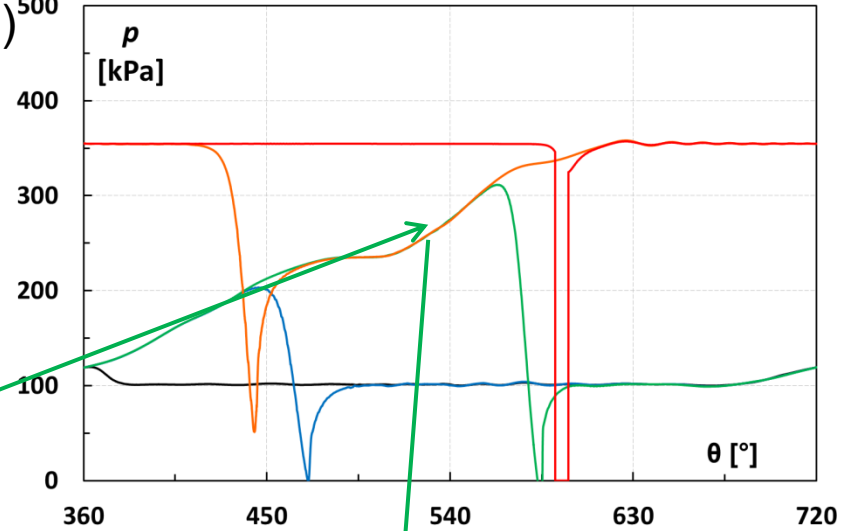
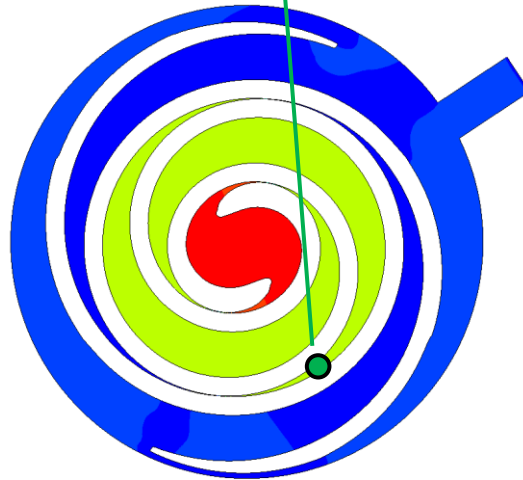
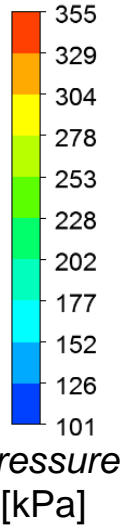
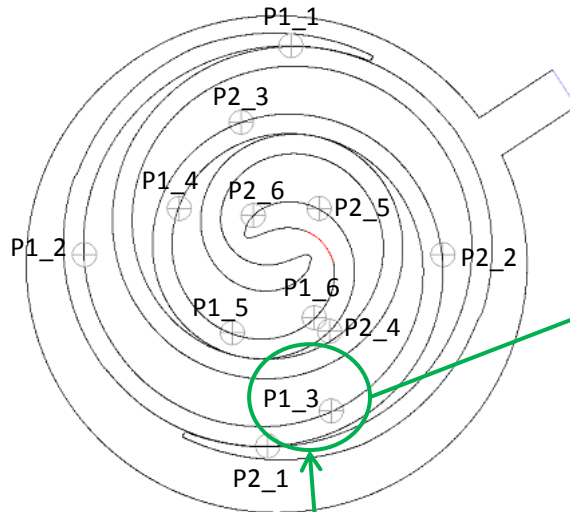
# Pressure control point (2)

## Compressor suction chamber 2



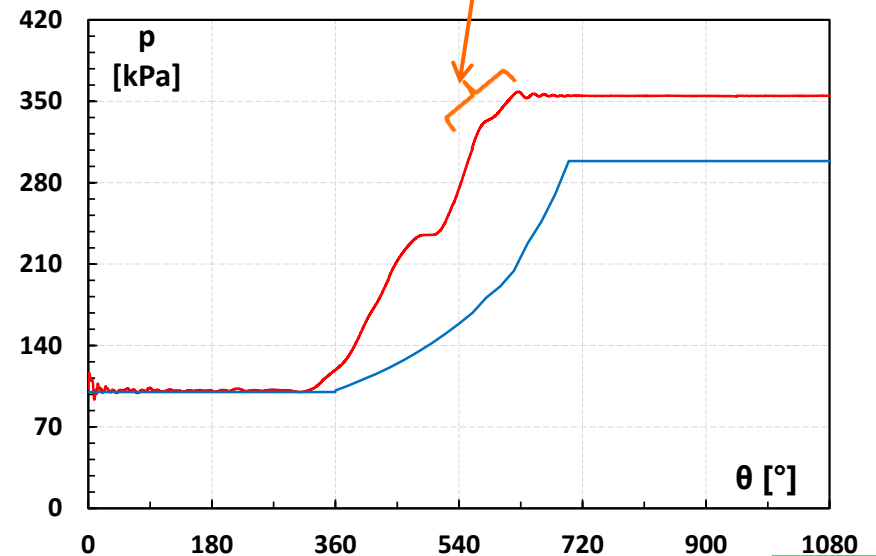
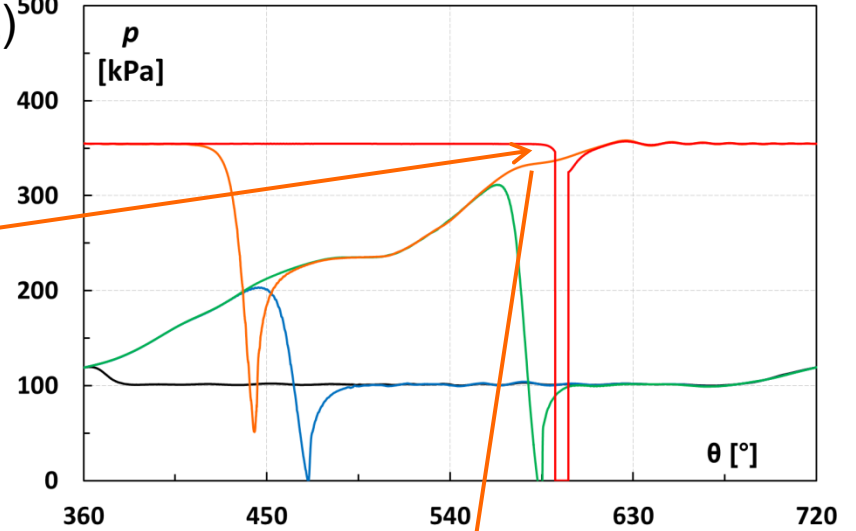
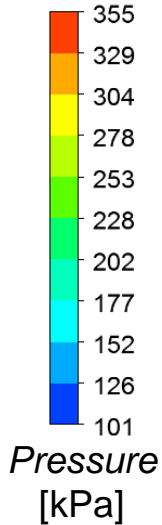
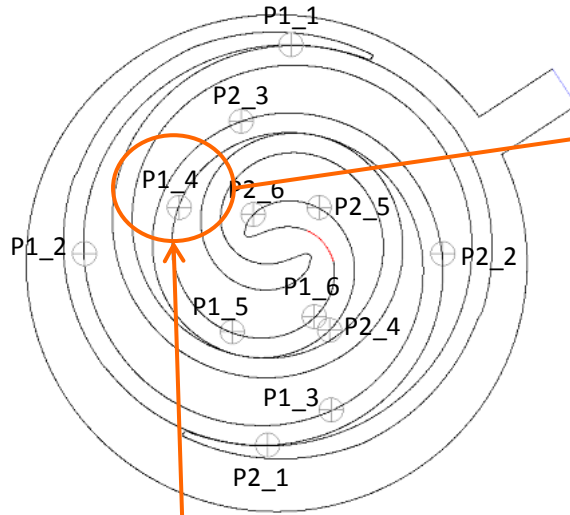
# Pressure control point (3)

## Compressor compression chamber (1)<sup>500</sup>



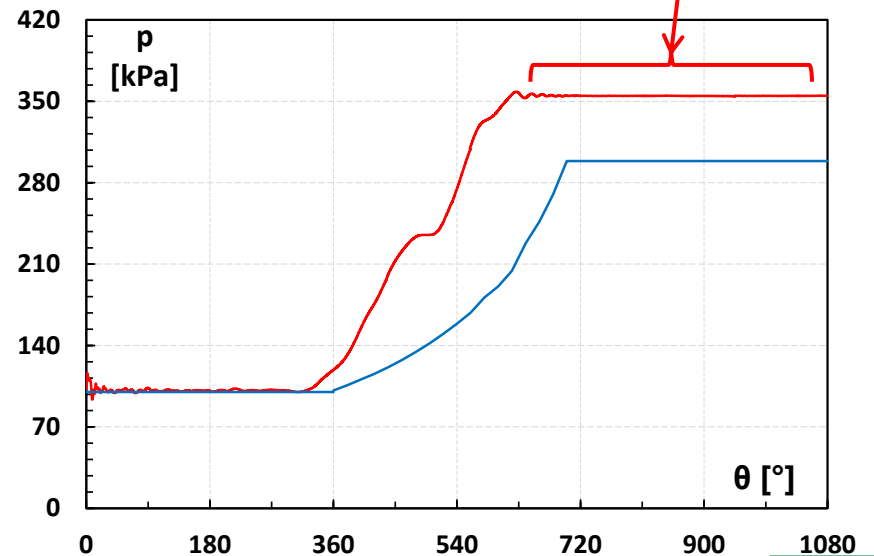
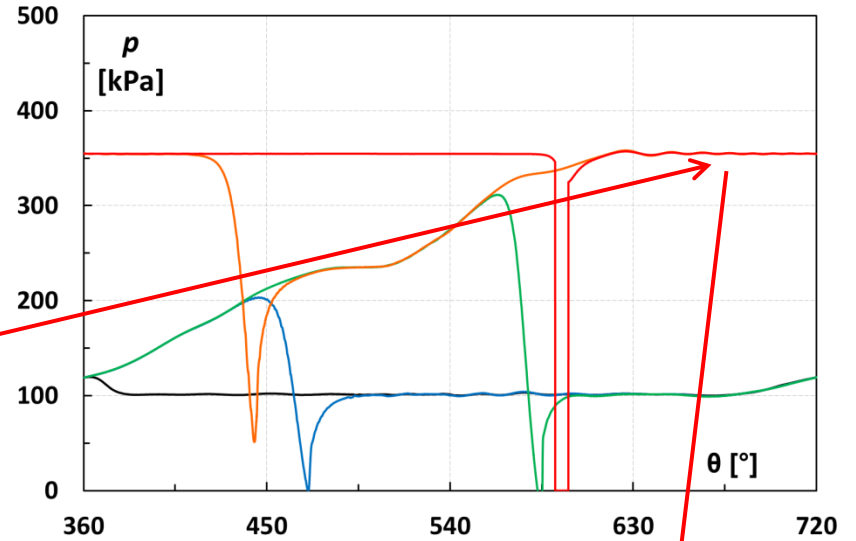
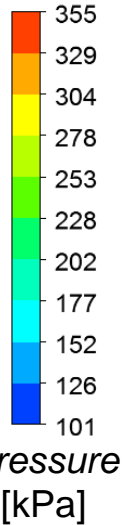
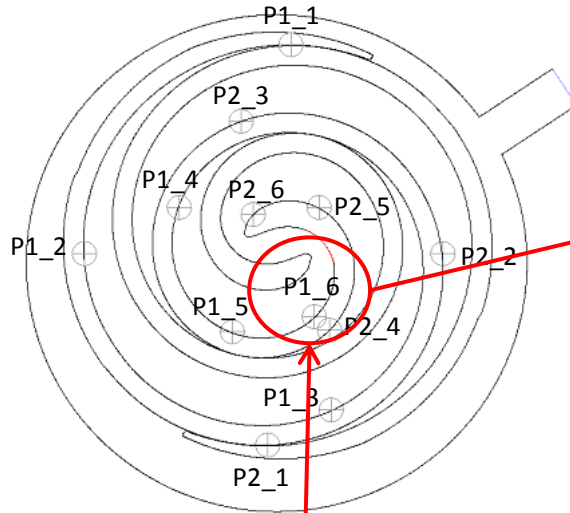
# Pressure control point (4)

## Compressor compression chamber (2)<sup>500</sup>



# Pressure control point (5)

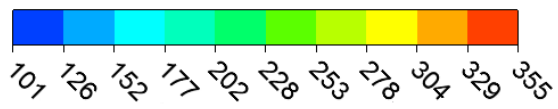
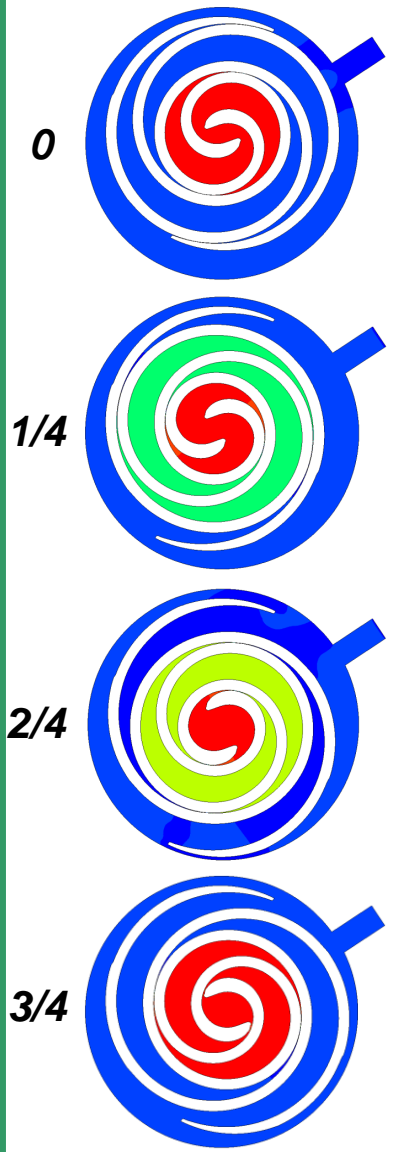
## Compressor discharge chamber



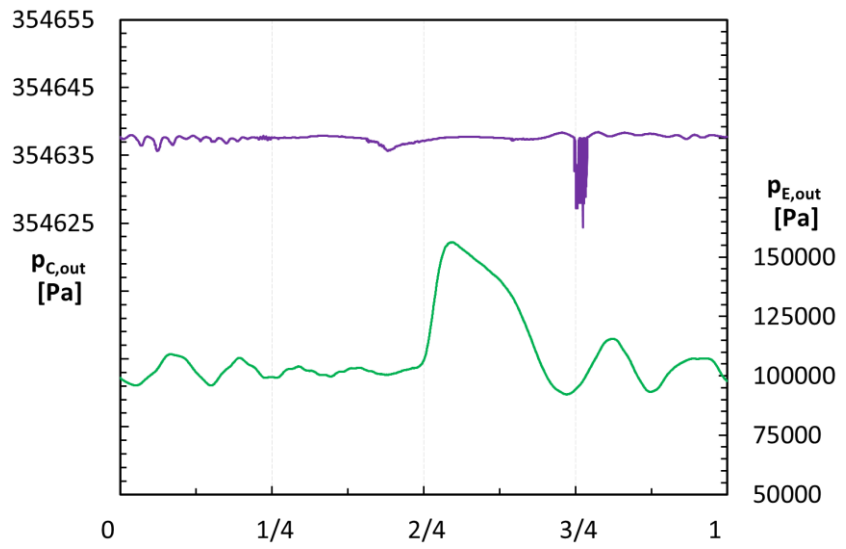


# CFD – Discharge pressure

## Compressor

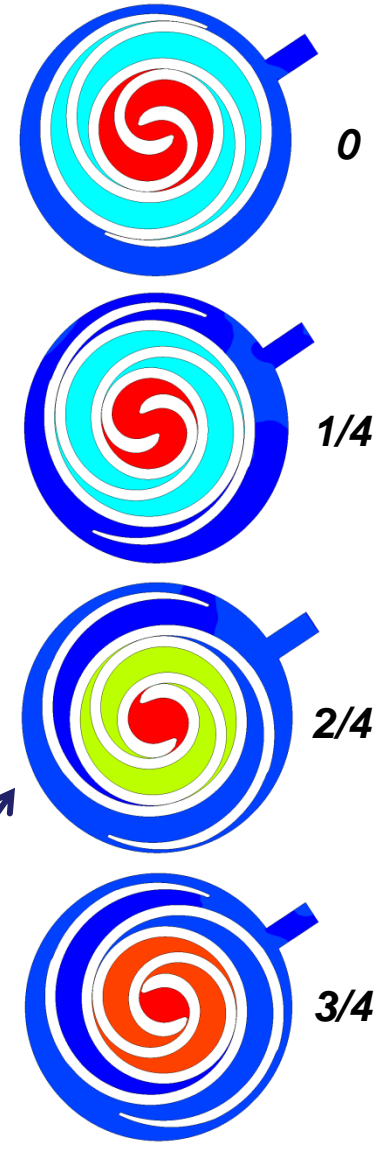


**Scroll expander** shows a more irregular trend, with **greater fluctuations** of the pressure value **at the exhaust**



Chambers with **different pressure** due to the **asymmetric inlet/outlet position**

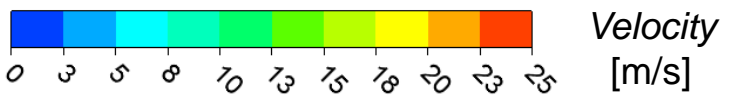
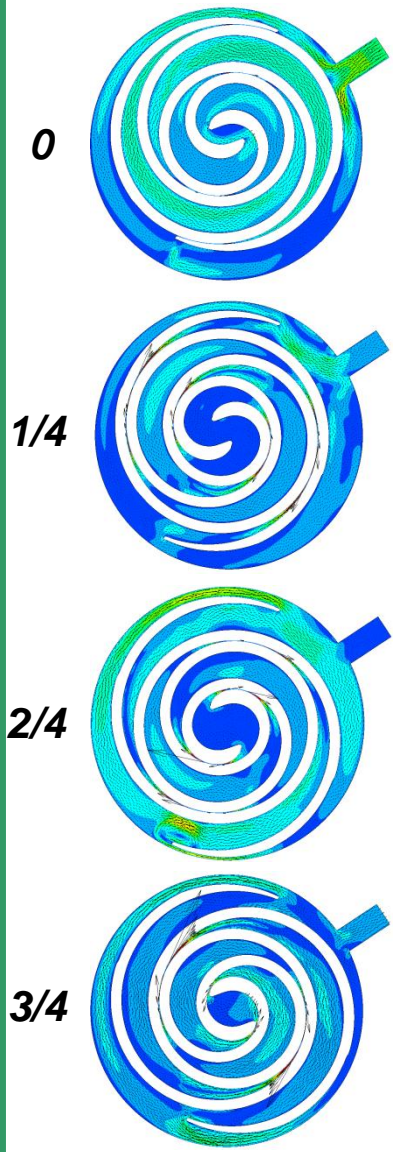
## Expander



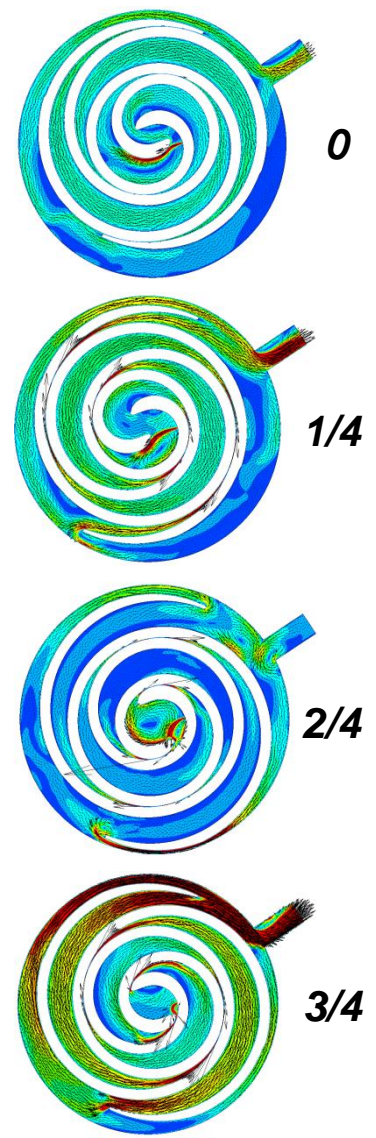


# CFD – Mass flow rate

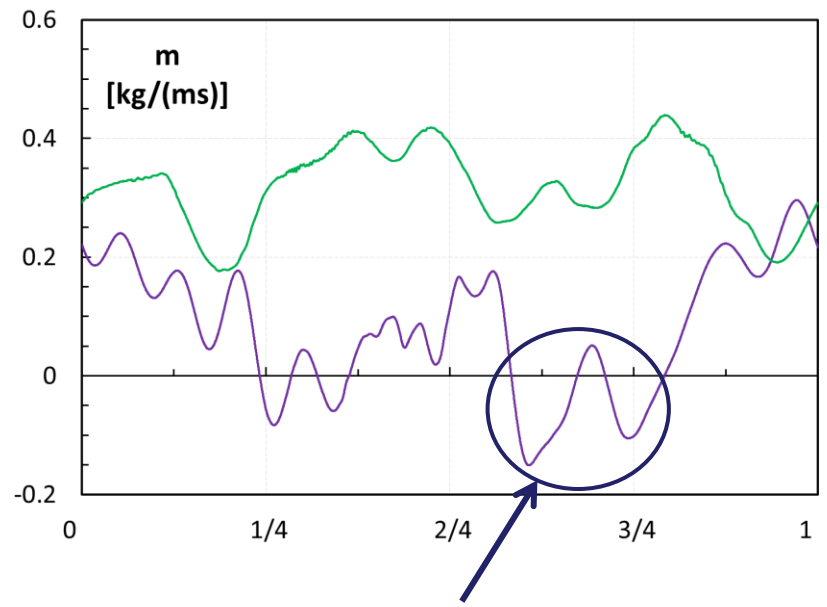
## Compressor



## Expander

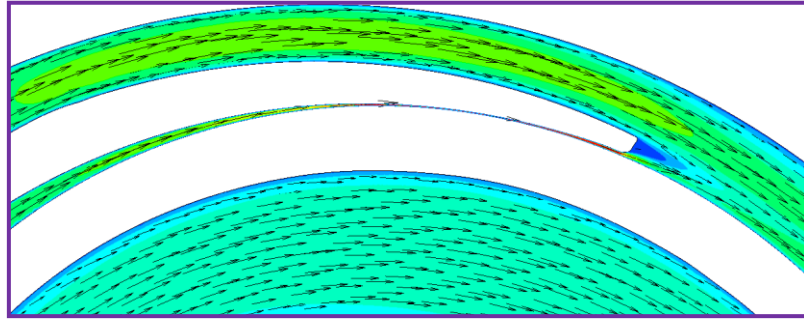
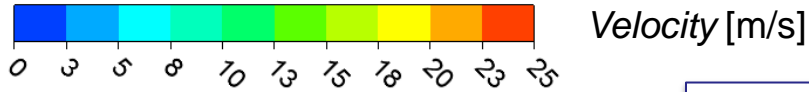


**Expander** provide **higher mass flow rate** than the compressor.  
This difference is due to the **flank gaps**

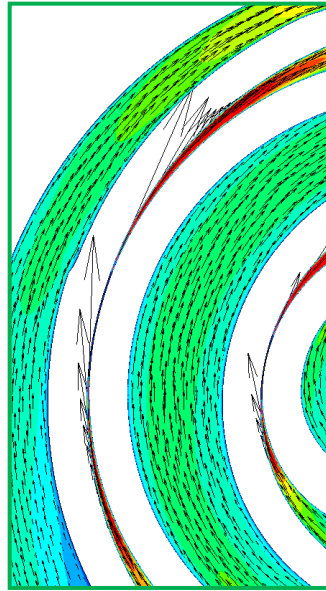


**Backflow** at the **inlet** for the **compressor**

# CFD – Mass flow rate (gaps)

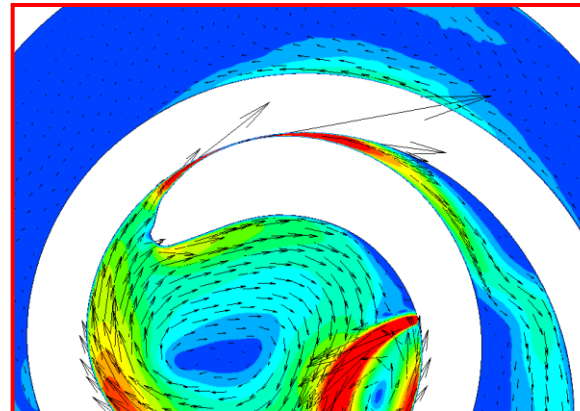


from the **discharge chamber** to the **outlet volume** (casing)

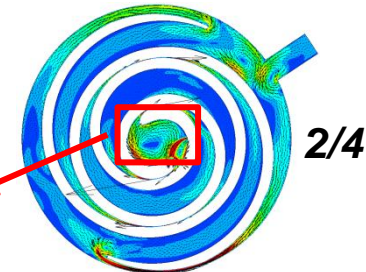
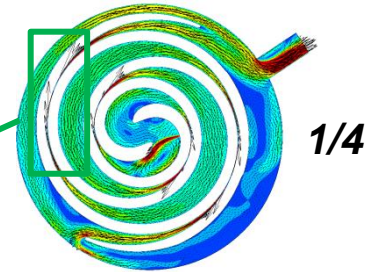
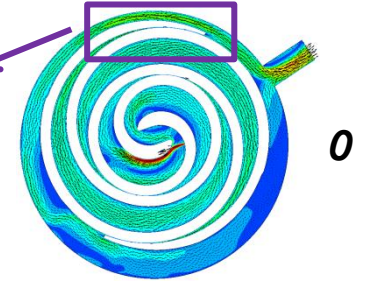


from the **expansion chamber** to the **discharge chamber**

from the **suction chamber** to the **expansion chamber**



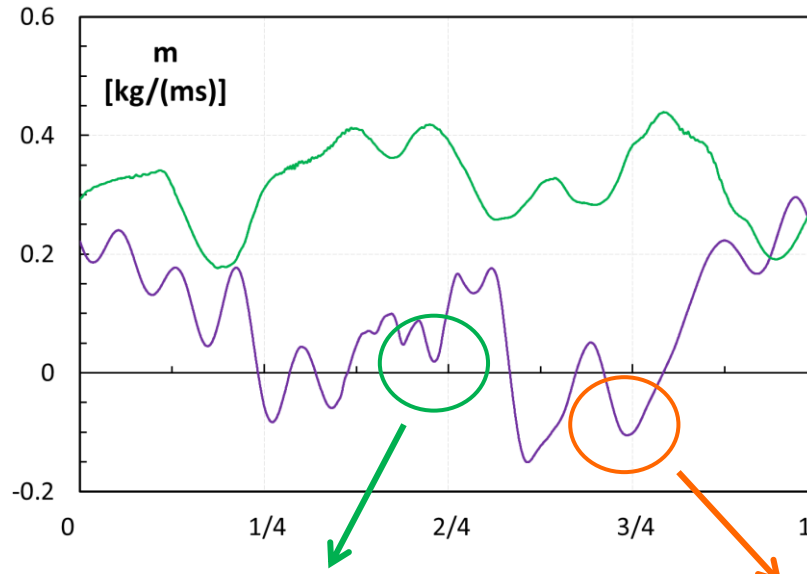
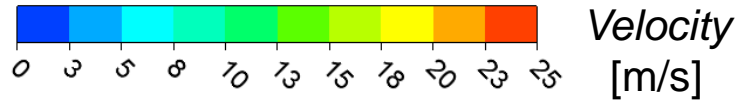
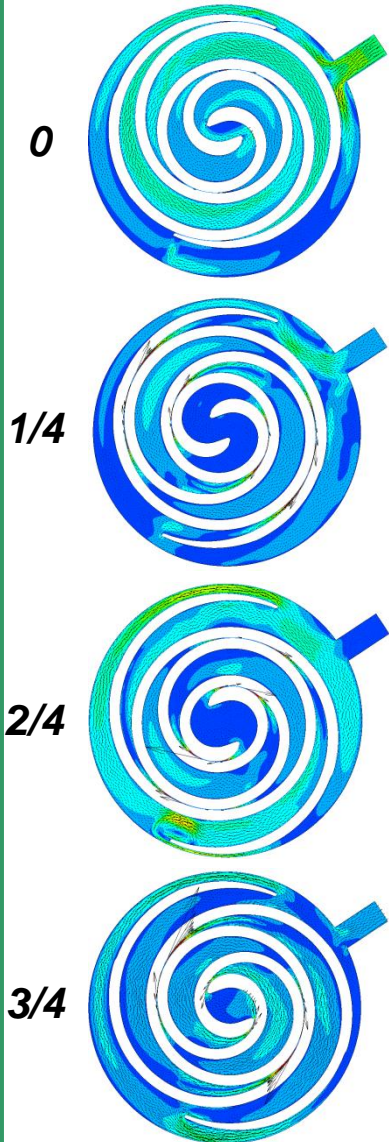
❖ Expander



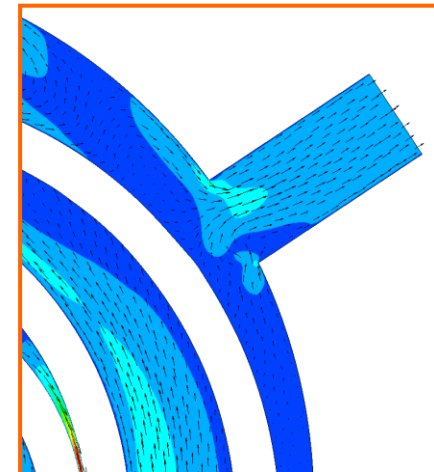
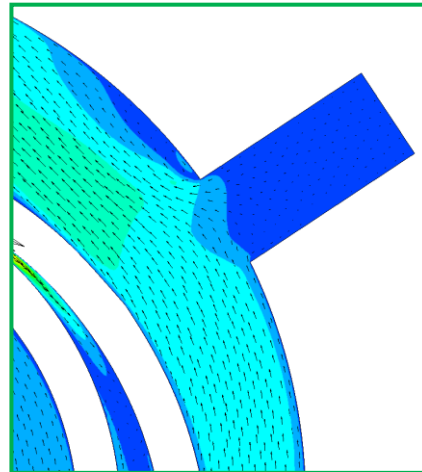


# CFD – Mass flow rate (backflow)

## ❖ Compressor



The **external volume** (casing) in the 2D numerical model seem to be **much smaller** than the necessary

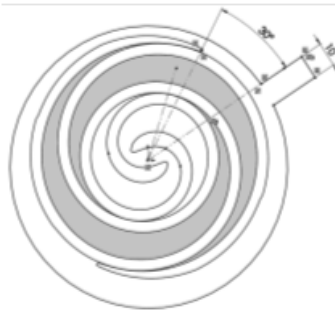


# Volumetric performance

- The **volumetric performance** was evaluated by the **geometric characteristics** (obtained from RE) and the **CFD results**

## ❖ Compressor

$Q_{out}$  is the outlet volumetric flow rate



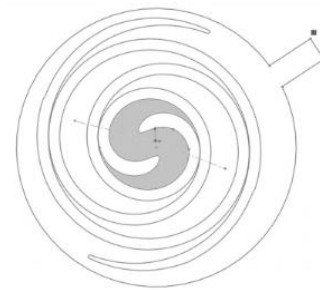
$$\eta_v = \frac{Q_{out}}{A_{in} n} = 0.29$$

$A_{in}$  is the area of the suction chambers

$n$  is the rotational speed

## ❖ Expander

$Q_{in}$  is the inlet volumetric flow rate



$$VFM_{ratio} = \frac{Q_{in}}{A_{in} n} = 3.06$$

- Low value** for  $\eta_v$  and **high value** for  $VFM_{ratio}$  (Volumetric Flow Matching ratio) is **closely related** to the value of the **flank gap** imposed between the fixed scroll and the moving scroll



# Conclusions

- An RE-CFD procedure together with a simplified thermodynamic model are used for analyze an commercial Scroll machine
- Thermodynamic simplified models can give reliable information on overall performance but largely fail in capturing detailed working features
- A comprehensive assessment of the machine performance can be obtained by the CFD simulations. In particular the velocity distributions and pressure field are highlighted
- A 2D numerical strategy which allow the study of the scroll in transient condition has been developed
  - ✓ 2D with organic fluids and fully 3D solutions are under development
- Information about the flow inside the scroll can be used to optimize the scroll design. In particular, the pressure fluctuations at the inlet and outlet port are closely related to vibrations and noise generated by the machine
  - ✓ These aspects play an important role in the case of household appliances, where the vibration and noise are as critical parameters as energy efficiency